Energy Proceedings
Vol 60, 2025
ISSN 2004-2965

Experimental study on the influence of wind turbine / wind farm on sand-dust transport

Gaosheng Ma[1,2*], Yuanxiang Song[1], Ye Wang[1], Yuben Bai[1], Minru Chen[1]

1 School of Green Energy and Storage, Lanzhou University of Technology, Lanzhou 730050, China;

2 Gansu Provincial Technology Center for Wind Turbines, Lanzhou 730050, China
(Gaosheng Ma: magsh@lut.edu.cn)

ABSTRACT

Wind energy development in sandy, Gobi, and desert regions presents significant advantages; however, the relationship between wind turbines/wind farms and dust transport remains unclear. This study pioneers the use of scaled single and multiple wind turbine models in a simulated aeolian environment within an atmospheric boundary layer wind tunnel. By employing particles of varying sizes and concentrations to represent sandstorms of different intensities, we investigate the impact of wind turbines/farms on dust transport and the effect of wind farm wakes on erodible surfaces. The results demonstrate that rotating turbine blades significantly obstruct dust transport, with tip vortices and the central vortex causing localized dust accumulation—particularly pronounced in upper tip vortex regions. Furthermore, dust accumulation occurs above wind farms, with the accumulation area expanding as particle size decreases. Operational wind farms promote dust deposition, with deposition rates decreasing as particle size increases. In the wake region, larger particles accumulate more readily, showing a positive correlation between accumulation and particle size. Additionally, large-scale wind farm wake effects effectively suppress dust emission.

Keywords: wind tunnel experiment, wind farm, sand-dust transport, dust particle size

NONMENCLATURE

Abbreviations	
CFD	Computational Fluid Dynamics
St	Stokes
WRF	Weather Research and Forecasting
LES	Large-eddy Simulation
ALM	Actuator Line Model
Symbols	
D	Diameter of Rotor
H_{hub}	Height of Hub
δ	ABL Thickness
R_s	Rotor Solidity
C_p	Power Coefficient
C_T	Thrust Coefficient
Re	Reynolds Number
λ	Tip Speed Ratio
Q	Sand Transport Flux
M	Sand-Dust Amount
S	Area of Sand Collection Cell
I	Variation factor of Sand-Dust transport rate
M	Sand-dust Amount

1. INTRODUCTION

Wind power has experienced remarkable growth over the past few decades. Currently, wind farm site selection is no longer confined to regions with superior wind resources and convenient grid access, such as coastal areas and inland plains, but has expanded to sandy, Gobi, and desert regions characterized by lower land costs and minimal human impact [1]. As massive structures standing within the atmospheric boundary layer, wind turbines interact with aeolian environments in complex ways. Their impact on regional dust transport processes, as schematically illustrated in Fig. 1, requires in-depth and systematic investigation.

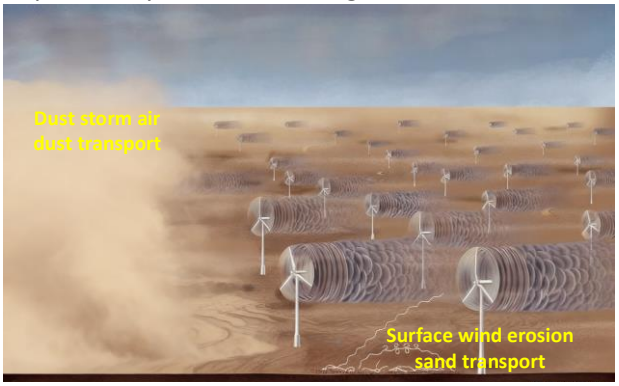

Fig. 1 Schematic diagram of interaction between wind farm and dust transport

Early research primarily focused on the interaction between wind turbines and inertial particles (e.g.,

This is a paper for the 5th Applied Energy Symposium and Forum: Renewable Energy Matrix (REM2025), Oct. 29-31, 2025, Yancheng, China.

raindrops, hailstones). Smith et al. conducted wind tunnel experiments injecting water droplets as inertial particles and observed droplet accumulation within the wind turbine wake. Their study emphasized the influence of droplet concentration on wake recovery and surrounding energy distribution [2]. Similarly, Travis et al. performed wind tunnel experiments using a porous disk as a turbulence generator to investigate the interaction between micron-sized water droplets and turbulence. Their results indicated that particles tend to accumulate in regions of higher turbulence intensity, and particle concentration affects the dissipation of turbulent kinetic energy [3]. He et al. employed CFD simulations to analyze velocity and pressure distributions in single-phase (air), liquid-gas, and solid-gas flows. Their findings revealed that while the velocity evolution trends in single-phase and two-phase flows are similar, the velocity gradients experienced by the blades in two-phase flows are significantly larger than those in single-phase flow [4]. However, the properties of these inertial particles differ from those of sand and dust particles. Although the Stokes number (St) varies across sandstorms of different intensities, it generally falls within the range of 2.0 to 35.9 [5].

The aerial transport of sand and dust in wind turbine/wind farm environments and the influence of dust on wake dynamics are fundamentally problems of particle-turbulence interactions within wake-particle two-phase flows. Therefore, understanding the underlying mechanisms governing dust behavior in wind turbine wakes requires returning to fundamental research on particle-turbulence interactions. As early as the late 20th century, Maxey theoretically derived and numerically demonstrated that particles tend to accumulate in regions of high strain rate and low vorticity, providing the first evidence that particle inertia can significantly enhance settling velocity [6]. Subsequently, Elghobashi et al. employed high-resolution direct numerical simulations to quantify the competing effects of gravity and inertia in turbulent particle dispersion [7]. Squires and Eaton et al. proposed that turbulence can selectively concentrate heavy particles, challenging the prevailing notion of "turbulence-enhanced mixing" [8]. Eaton and Fessler further established the universal mechanism of preferential particle concentration in turbulence and identified the Stokes number as the key parameter governing this behavior [9]. Lazaro et al. were the first to experimentally observe a three-zone structure in droplet dispersion layers, where centrifugal effects induced by large-scale vortices caused size-selective migration—small droplets being drawn into vortex cores while larger droplets were expelled to vortex peripheries due to inertial forces [10]. These profound insights into particle transport in turbulence have significantly advanced our understanding of how wind turbine wakes influence dust transport and dispersion.

In recent years, the research team focusing on wind-blown sand and wind turbine interactions at Lanzhou University of Technology (the authors of this paper) has conducted numerical simulations specifically targeting sand-laden environments. Wang et al. employed Large Eddy Simulation (LES) combined with the Actuator Line Method (ALM). Their findings indicate that turbine wake turbulence significantly weakens the correlation between dust concentration (primarily PM10 and PM30) and flow velocity, with the correlation coefficient decreasing by up to 16.6%. Concurrently, the wake enhances the vertical turbulent diffusion of dust, particularly for larger particles such as PM30 [11]. Ma et al. utilized the Multiphase Particle-in-Cell method integrated with an actuator line model, extending the investigated particle size range. Their simulation results demonstrate distinct distribution patterns for different particle sizes, with smaller particles exhibiting more homogeneous dispersion. Sand particles tend to accumulate around tip vortices and the peripheries of low-vorticity vortex cores, forming a "network-like" structure. The wind turbine substantially impedes sand transport, with the average sand-blocking rate initially increasing and then decreasing along the wake distance, reaching a peak value of 67.55%. Furthermore, the wind turbine induces premature settlement of sand particles, resulting in a "triangular" deposition pattern on the ground within the wake projection. The deposition mass of fine particles (e.g., 10μm) increased significantly by 20.20%, while coarse particles showed minimal change or even a reduction in deposition due to inertial effects. Proper Orthogonal Decomposition (POD) analysis reveals that dust alters large-scale vortex structures, leading to a reduction in wake scale. Dust suppresses energy entrainment by large-scale structures while promoting energy activity in smaller-scale structures. Within the wake region, both the concentration and size of airborne dust particles are smaller compared to the lateral sides. Dust exhibits complex meandering motions in the wake, with trajectory complexity increasing as particle size decreases. The presence of the wind turbine promotes premature sand settlement, similarly forming a triangular deposition pattern in the downstream wake region [12, 13].

At the wind farm scale, the environmental impacts of large-scale wind farms have attracted increasing attention. Early studies primarily focused on their effects on temperature, surface microclimate, and humidity [14]. In recent years, several researchers have begun investigating the influence of wind farms on the dispersion and deposition of atmospheric pollutants. For instance, Ruan et al. systematically evaluated the direct and indirect impacts of wind farms in Zhangjiakou on air quality. Their results indicated that wind farm deployment in Chengde directly affected $PM_{2.5}$ concentrations in Beijing, leading to a net increase of 0.08% [15]. Similarly, based on mesoscale simulations of gigawatt-scale wind farms in Zhangbei County, Hebei Province, Wang revealed that large-scale wind farms exert significant and persistent local influences, simultaneously affecting the local atmospheric boundary layer and indirectly modulating the dispersion of air pollutants [16]. Mataji's numerical simulations further indicated that wind farms can act as physical barriers, impeding dust movement and resulting in a 23.3% increase in $PM_{2.5}$ deposition and a 34.2% increase in PM_{10} deposition [17]. Wang Qiang et al. employed a WRF-CMAQ model coupled with wind farm parameterizations to assess the impact on air quality. Their study demonstrated that wind farms can promote the redistribution of atmospheric pollutants, leading to regional dispersion and transport, while also exhibiting distinct seasonal variations [18]. Mo et al. utilized the WRF-Chem model to simulate nitrogen dioxide concentrations around large wind farms. The results showed elevated concentrations at the upwind fringe and the near-downwind transition zone of the wind farms, with relatively higher pollutant levels in the upwind region compared to scenarios without wind farms [19]. Collectively, these numerical studies demonstrate that wind farm layouts significantly influence the transport of dust and other pollutants.

Previous studies have predominantly focused on the interactions between meteorological particles such as raindrops, water droplets, and hail with fluid flows, while notable distinctions remain in relation to wind-sand two-phase flows. To address the scientific issues concerning the interaction between wind-sand environments and wind turbines, our research team has systematically investigated the distribution characteristics of wind-blown sand, settling behavior, and the wake turbulence structures of wind turbines. However, most of the existing findings rely on numerical simulation methods. In this field, beyond field observations, no physical simulations of wind farms under wind tunnel experimental conditions have been reported to date. Therefore, based on a summary of prior numerical results, our team has further employed experimental approaches to validate the corresponding numerical simulations. This study employs scaled wind turbine models arranged in staggered arrays to simulate wind farm conditions within a sand-laden environmental wind tunnel. This constitutes the first experimental investigation into the mutual interactions between wind turbines/wind farms and dust transport processes.

2. MATERIAL AND METHODS.

Two scaled-down models with distinct scaling ratios were designed based on the unility-turbine 5-MW reference horizontal-axis three-bladed wind turbine. The smaller-scale model was developed for wind farm simulations, while the larger-scale model was intended for single-turbine studies. The blade design utilized the SG6050 airfoil, selected for its superior aerodynamic efficiency and reliability under low-Reynolds-number conditions. The similarity parameters for both models are summarized in Table 1.

Table. 1 Geometric parameters and similarity ratio of wind turbine model

	D	H_{hub}	δ/H_{hub}	R_s	C_p	C_T	Re	λ
Utility-scale turbine	100	118	1.67	4-9%	0.4	0.85	8.1×10^6	6.4
Model Turbine 1	0.15	0.18	1.67	8%	0.205	0.7	5×10^4	7.36
Model Turbine 2	0.44	0.3	1.67	8%	0.29	0.78	1.09×10^5	7

The two scaled wind turbine models are shown in Figure 2.

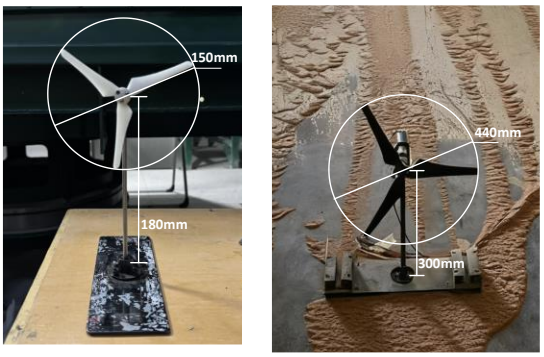

a. Model Turbine 1 **b. Model Turbine 2**

Fig. 2 Wind turbine model

The experiments were conducted in the environmental wind tunnel laboratory at the Gansu Wind Turbine Engineering Technology Research Center of Lanzhou University of Technology. An aerial view of the wind tunnel is presented in Figure 3. It is a U-shaped boundary layer wind tunnel with a total length of 25.4m, featuring a test section measuring 17m in length, 2m in

width, and 2m in height. The designed wind speed range of the tunnel is 1–30m/s, with a background turbulence intensity below 1%. The facility is equipped with a dedicated sand-dust injection system capable of adjustable concentration. The sand-dust injection port is illustrated in Figure 4.

Fig. 3 Wind tunnel *Fig. 4 Sand and dust release port*

an exponential distribution pattern, while deviations from the exponential distribution are observed in the near-bed region. To eliminate the influence of the sand sampler's inherent collection performance on the experimental results, all data collected by the sand samplers in this experiment were processed by converting them into relative values based on baseline data obtained under empty wind tunnel conditions. This approach effectively controls the experimental variables to changes in wind turbine layout within the wind farm and variations in the distance from the wind turbine

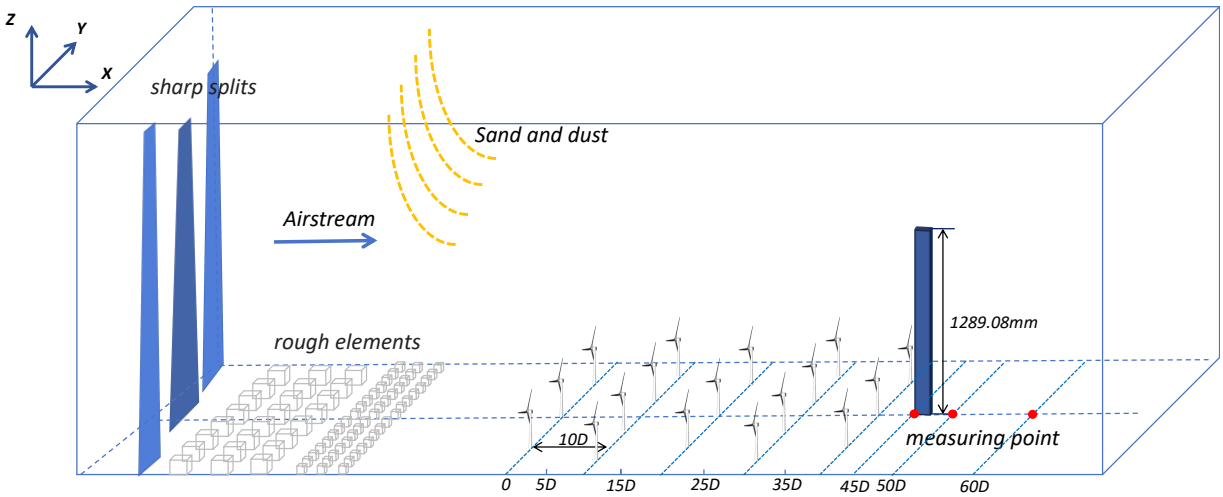

Fig. 6 Experimental condition diagram of wind farm

The neutral atmospheric boundary layer was simulated using a combination of spires and roughness elements. For sand collection measurements, a device based on the structural design of the Liu-type sand sampler [20] was employed, with a collection range of 34.84-1289.88mm. As shown in Figure 5, each collection unit has a cross-sectional area of 30mm × 34.84mm. Since this study specifically focuses on sand collection data behind the wind farm and derives relative sand collection and transport effects at different intra-farm locations through comparative calculations, an intrusive measurement approach was adopted for sand collection quantification.

Regarding the sand sampler device, Ni et al. employed a Liu-type sand sampler to measure the vertical distribution of sediment transport flux under two different particle size conditions in a wind tunnel environment. Experimental results indicate that the vertical distribution pattern of sediment transport for finer particles is more sensitive to variations in wind speed, whereas the distribution pattern of coarser particles is less influenced by wind speed changes. Under both sand grain conditions, the upper segment of the vertical distribution of sediment transport conforms to wake region[21], thereby ensuring the validity of data comparison and the reliability of experimental results.

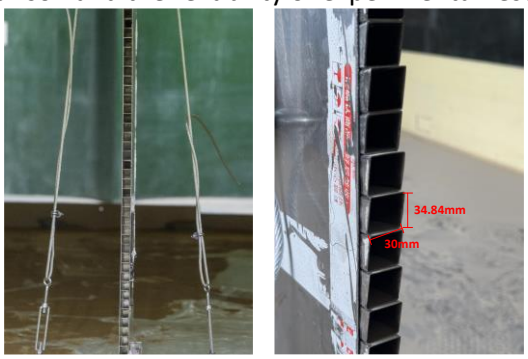

a. Integrated graph **b. Local details**

Fig. 5 Sand sampler local diagram

Natural sand from the Tengger Desert was selected as the sand source. Through sieving, three monodisperse sand samples with particle sizes of 200μm (representing severe black storms from erodible desert surfaces, St>50), 100μm (representing strong sandstorms at desert margins, St>10), and 50μm (representing blowing sand weather, St≈1), along with a polydisperse mixed sand sample, were prepared, constituting four test conditions. All experiments were conducted at a constant wind speed of 11.3m/s, with each test condition

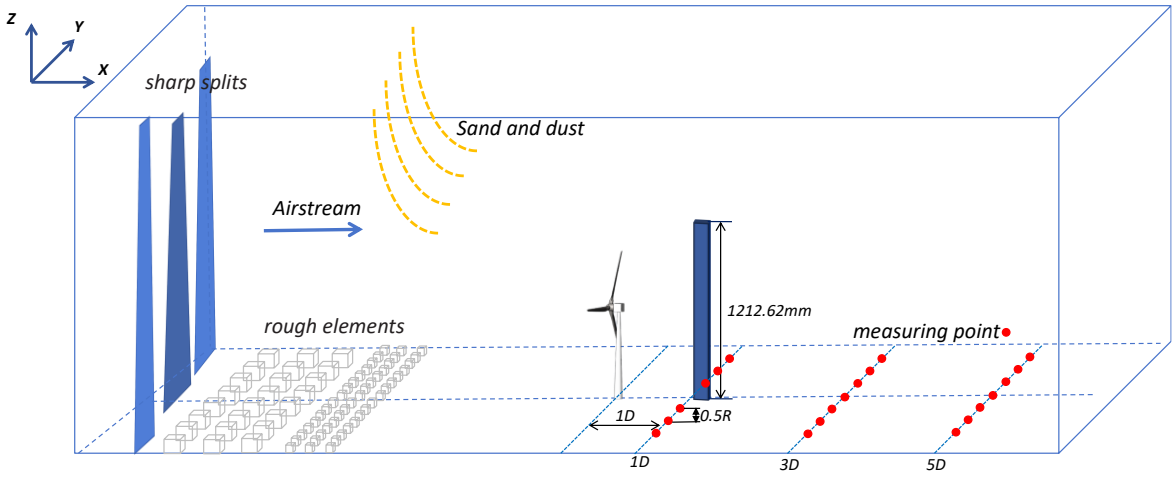

Fig. 7 Experimental condition diagram of wind turbine

lasting 300s. The wind farm layout initially consisted of five rows of turbines, with the sand sampler position held constant. The number of turbine rows was then progressively reduced, enabling indirect measurement at different intra-wind-farm locations, culminating in a final configuration with no turbines (i.e., the background sand-laden environment). A schematic of the experimental design is shown in Figure 6. For each layout configuration, measurement points were established at typical locations within the wind farm and at downstream positions of 5D, 10D, and 20D (specifically at 45D, 50D, and 60D in the figure), allowing for systematic collection of sand particle data. For the single wind turbine configuration, the wind tunnel speed was set to 7m/s, corresponding to a tip-speed ratio (λ) of approximately 6.4, representing the rated operational condition. A sand environment with 100μm particles was used. Measurement planes were selected at vertical axial (i.e., transverse) cross-sections located 1D, 3D, and 5D downstream of the rotor. At each cross-section, measurements were taken at seven radial positions: r/R=0, r/R=±0.5, r/R =±1.0, and r/R=±1.5. The distribution of measurement points is shown in Figure 7, with a measurement duration of 140 s for this configuration.

It should be specifically noted that when simulating environments with fine sand particles, the wind tunnel speed was appropriately reduced to accurately reproduce the settling behavior of fine particles observed in the actual atmosphere. Details of all test conditions are provided in Table 2.

Measurements of the sand transport rate under empty tunnel conditions reveal that the incoming sand transport rate follows an exponential decay distribution with height. Furthermore, the vertical distribution becomes increasingly concentrated near the surface with increasing sand particle size. The resulting sand transport flux distributions are shown in Figures 8 and 9. A schematic summarizing the experimental test conditions is provided in Figure 10.

Table. 2 Details of experimental conditions

	50 μ m	100 μ m	200 μ m	Mixed
One row	45D	45D	45D	45D
Two rows	45D	45D	45D	45D
Three rows	45D	45D	45D	45D
Four rows	45D	45D	45D	45D
Five rows	45D,50D,60D	45D,50D,60D	45D,50D,60D	45D,50D,60D
Empty field	45D,50D,60D	45D,50D,60D	45D,50D,60D	45D,50D,60D
One		1D,3D,5D		

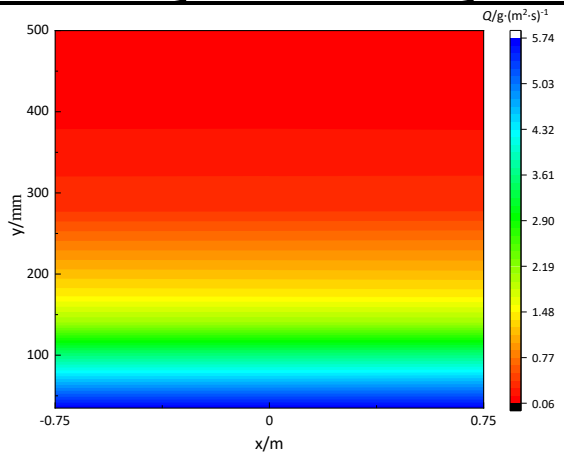

Fig. 8 Distribution of incoming sand-dust transport rate (vertical direction)

The sand transport flux is defined by Equation (1):

$$Q = \frac{M}{S \cdot t} \tag{1}$$

Where Q is the sand transport flux at a given height (unit: g/(m²·s)), M is the mass of collected sand at the specific height (unit: g), S is the cross-sectional area of the

collection unit (unit: m²), and t is the sand collection duration (unit: s).

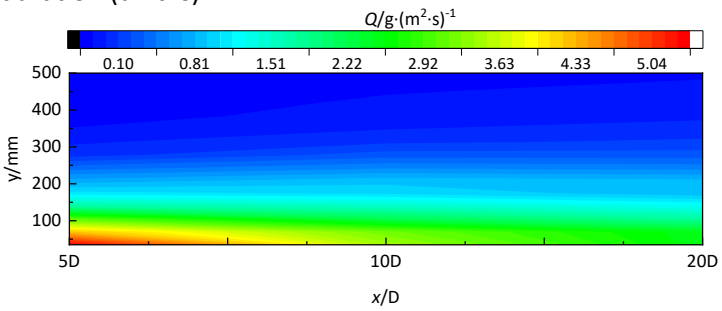

Fig. 9 Distribution of incoming sand-dust transport rate(spanwise)

Fig. 10 Experimental condition diagram

The transport rate variation factor is defined as:

$$I = \frac{M_0 - M_1}{M_0} \quad (2)$$

Where I is the dimensionless transport rate variation factor, M_0 is the mass of sand collected at a specific height without the wind turbine (unit: g), and M_1 is the corresponding mass collected with the wind turbine present (unit: g). Positive values of I indicate sand-dust retention, while negative values indicate enhanced sand suspension.

3. RESULTS AND DISCUSSION

3.1 Effects of wind turbine on sand-dust transport

To investigate the sand-dust transport characteristics in the wind turbine wake at the rated tip-speed ratio (λ=6.4), Figure 11 presents the sand transport flux distributions at transverse cross-sections located 1D, 3D, and 5D downstream. The results demonstrate that the combined effects of rotor-induced blockage, particle collisions, and downward-tip vortices lead to significant accumulation of sand transport flux near the bed, exhibiting a bimodal distribution along the wake centerline. Influenced by the clockwise rotation of the rotor (from the inflow perspective), the accumulation zone displays an asymmetric distribution, with the peak flux on the left side exceeding that on the right. The sand transport flux distribution above the hub height further reveals that areas of dust accumulation closely correspond to the trajectories of the tip vortices, manifesting as distinct arc-shaped high-concentration bands with cluster structures in the transverse cross-sections. Additionally, sand accumulation is also observed in the central vortex region, a feature most pronounced at the 1D cross-section.

Due to complex energy exchange between surface turbulence and downward-tip vortices, large-scale turbulent disturbances continuously weaken the coalescence capacity of tip vortices, resulting in a less pronounced enrichment effect on sand particles. As the wake develops further downstream, both the tip vortices and central vortex exhibit diminished dust accumulation effects at the 3D location, with the central vortex demonstrating more significant attenuation. By 5D and beyond, as the wake progressively recovers and vortex structures continuously dissipate, their capacity to confine sand particles markedly decreases. This ultimately leads to widespread dispersion of sand across the rotor-swept area, achieving a more uniform distribution pattern.

3.2 Influence of wind farm on sand-dust transport

The study first examined and calculated the transport rate variation factor under various particle size conditions. As shown in Figure 12, the region above the wind farm generally exhibited transport rate variation

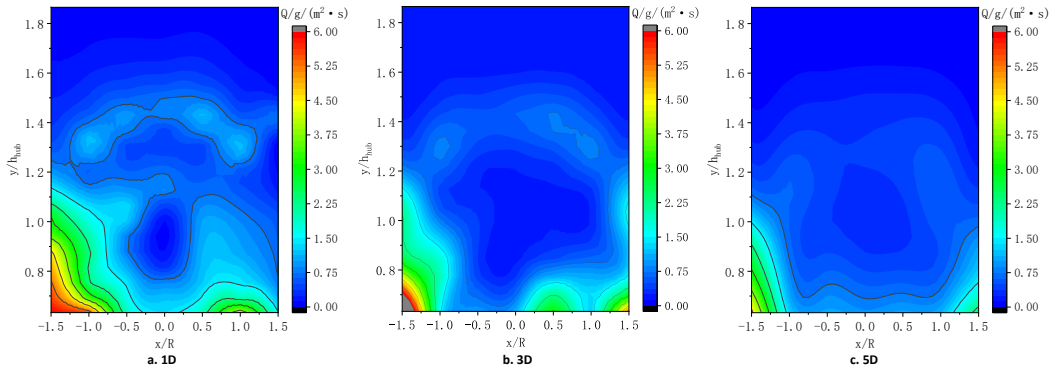

Fig. 11 Sand-dust transport flux distribution indifferent sections

factor values less than zero, indicating net dust accumulation in this area. This phenomenon is primarily attributed to aerodynamic effects such as upper tip vortices and rotor collisions, which lead to the formation of dust accumulation zones above the wind farm for different particle sizes. Quantitative analysis reveals that the spatial extent of the accumulation zone decreases significantly with increasing particle size: the accumulation area for mixed-size particles is 70.83% smaller than that for the 100-μm case. Furthermore, under all test conditions, the dust concentration within the accumulation zone gradually decreases with increasing horizontal distance. Taking 100-μm particles as an example, at the 600 mm height, the dust concentration at the 50D location decreased by 22.68% compared to that at the 15D location, demonstrating a distinct streamwise diffusion and settling trend.

in this region. The turbulent kinetic energy and velocity deficit provided by the wind farm wake further promote kinetic energy dissipation and eventual deposition of these particles.

Within the interior region of the wind farm, constrained by the limited development space for downward-tip vortices and the mutual interference of flows between multiple turbines, enhanced dust deposition was observed under all test conditions. As shown in Figure 13, with the expansion of the wind farm scale (i.e., number of turbine rows), the internal dust deposition exhibited an overall increasing trend. Notably, the deposition efficiency demonstrated a conspicuous particle-size dependence, showing more significant enhancement for finer particles. Taking 50-μm particles as an example, after deploying five turbine rows, the deposition mass increased by approximately

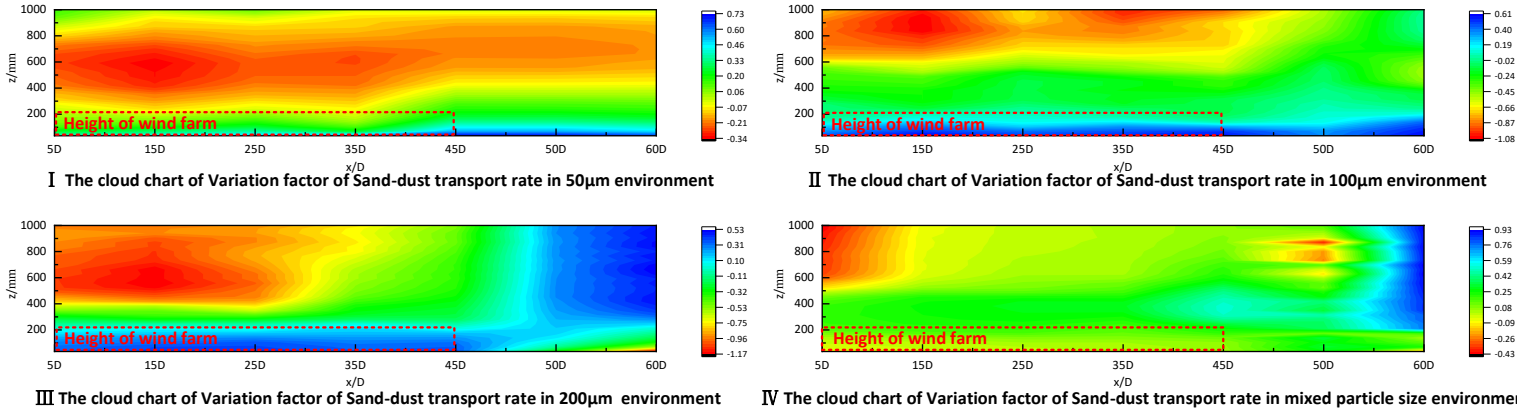

Fig. 12 Variation factor of Sand-dust transport rate distribution map

Within the wind farm wake-affected area, this study observed significant deposition of both 200μm and mixed-size particles. Specifically, with turbines installed up to the 60D location, the deposition mass of 200μm particles increased by 41.96%, while that of mixed-size particles increased by 56.25%. This phenomenon can be attributed to the superposition of multiple turbine wakes in the lee side of the wind farm, which induces a gradual streamwise velocity deficit and a sustained enhancement of turbulence intensity [22]. Such flow characteristics provide additional kinetic energy to saltating particles on one hand, and enhance dust transport and mixing on the other. This observation aligns with classical aeolian physics: larger particles are more susceptible to initiation of saltation under wind forcing [23]. It is noteworthy that the deposition efficiency is closely related to particle size, with larger particles exhibiting more pronounced settling within the wind farm wake. Particularly for particles exceeding 200μm in diameter, a greater proportion tend to deposit

56.86% compared to the scenario without wind farms, convincingly demonstrating the flow field within wind farms efficiently promotes the deposition of fine particulate matter.

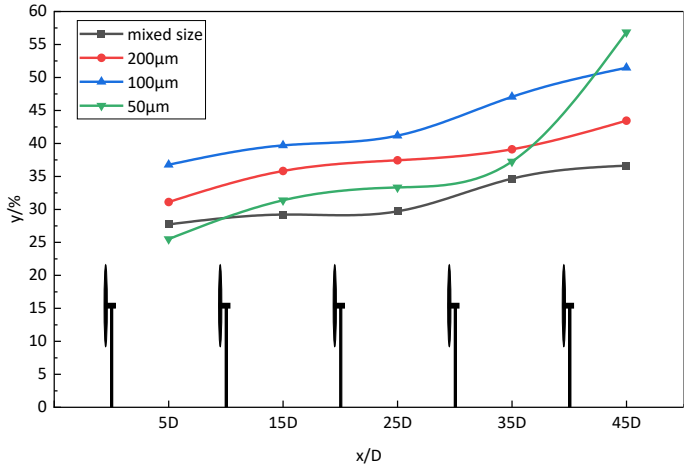

Fig. 13 The schematic diagram of dust deposition ratio in wind farm

This study reveals that while serving as producers of green energy, wind farms simultaneously play a crucial role as ecological regulators. This finding enriches the concept of synergistic development by demonstrating that through scientific planning and design, wind farms can achieve the dual objectives of clean energy output and regional sand control. The results highlight their significant potential as strategic infrastructure capable of delivering both energy and ecological services.

4. CONCLUSIONS

This study aims to elucidate the impact mechanisms of large-scale wind farms on wind-blown sand transport in desert environments, with particular focus on their effects on the distribution and migration of different particle sizes during sandstorms. The key experimental findings are as follows:

(1) During turbine operation, wake evolution directly modifies dust transport characteristics. Both tip and central vortices in the wake region exhibit significant dust accumulation effects. The upper tip vortices form distinct arc-shaped dust concentration bands in transverse cross-sections, demonstrating stronger accumulation capability than the central vortex.

(2) Under combined aerodynamic effects including upper tip vortex interactions and rotor collisions, a stable dust accumulation zone forms above the wind farm. Experimental results confirm this accumulation zone's spatial extent is particle-size-dependent, with finer particles exhibiting the most extensive accumulation area due to superior flow-following capability.

(3) Within the wind farm wake-affected region, larger particles experience shortened airborne duration due to faster settling velocities. Concurrently, turbulent fluctuations in the wake provide additional kinetic energy for particle saltation. These combined mechanisms enhance the deposition of coarse particles, resulting in a significant positive correlation between deposition mass and particle size.

(4) Inside the wind farm, turbine-turbine interactions generate complex turbulent structures that significantly promote dust sedimentation. This enhanced deposition exhibits clear particle-size dependence, with finer particles showing higher deposition efficiency. Consequently, the internal deposition mass demonstrates a negative correlation with particle size.

ACKNOWLEDGEMENT

This work was supported by the National Key Research & Development Program of China (Grant Nos. 2022YFB4202104).

REFERENCE

[1] Y. Wang, R. Wang, K. Tanaka, et al. Accelerating the energy transition towards photovoltaic and wind in China. Nature. 2023;619 (7971):761-767.

[2] Sarah E. Smith, Kristin Travis, Henda Djeridi, et al. Dynamic effects of inertial particles on the wake recovery of a model wind turbine. RENEWABLE ENERGY. 2020;164 (0):346-361.

[3] Kristin Travis, Sarah E. Smith, Laure Vignal, et al. Characterization of coupling between inertial particles and turbulent wakes from porous disk generators. JOURNAL OF FLUID MECHANICS. 2022;933 (0):A42-A42.

[4] P. He, N. Chen, D. Hu. Study of Wake Characteristics of a Horizontal-Axis Wind Turbine within Two-Phase Flow. Key engineering materials. 2011;474-476 (0):811-815.

[5] Z. Song, J. Wang, S. Wang. Quantitative classification of northeast Asian dust events. Journal of Geophysical Research Atmospheres. 2007;112 (D4)

[6] Martin Maxey. The gravitational settling of aerosol particles in homogeneous turbulence and random flow fields. JOURNAL OF FLUID MECHANICS. 1987;174 (0):441-465.

[10] S. Elghobashi, G. C. Truesdell. Direct simulation of particle dispersion in a decaying isotropic turbulence. JOURNAL OF FLUID MECHANICS. 1992;242 (0):655-700.

[7] Kyle D. Squires, John K. Eaton. Preferential concentration of particles by turbulence. Physics of Fluids A Fluid Dynamics. 1991;3 (5):1169-1178.

[8] John K. Eaton, John R. Fessler. Preferential concentration of particles by turbulence. INTERNATIONAL JOURNAL OF MULTIPHASE FLOW. 1994;20 (0):169-209.

[9] B. J. Lázaro, Juan C. Lasheras. Particle dispersion in a turbulent, plane, free shear layer. Physics of Fluids A Fluid Dynamics. 1989;1 (6):1035-1044.

[10] Z. Ruan, X. Lu, S. Wang, et al. Impacts of large-scale deployment of mountainous wind farms on wintertime regional air quality in the Beijing-Tian-Hebei area. ATMOSPHERIC ENVIRONMENT. 2022;278 (0):119074-119074.

[11] Y. Wang, R. Guan, P. Lu, et al. Large-eddy simulation of dust transport and coherent structures in a wind turbine wake. Physics of Fluids 1 September 2025; 37 (9): 095203. https://doi.org/10.1063/5.0289853

[12] G. Ma, H. Han, Y. Li, et al. Numerical and experimental study of the effects of wind turbine operation on sand-dust transport characteristics. Science China-Physics Mechanics & Astronomy. 2024;67 (4):97-113.

[13] G. Ma, Q. Zheng, D. Li, et al. (in press). Study of the Interaction between Wind Turbine Wake and Sand Transport in Sand-Wind Environment. Renewable Energy. 2025. doi:10.2139/ssrn.4979940
[14] Somnath Baidya Roy, Stephen W. Pacala, R. L. Walko. Can large wind farms affect local meteorology? Journal of Geophysical Research Atmospheres. 2004;109 (D19)
[15] Z. Ruan, X. Lu, S. Wang, et al. Impacts of large-scale deployment of mountainous wind farms on wintertime regional air quality in the Beijing-Tian-Hebei area. ATMOSPHERIC ENVIRONMENT. 2022;278 (0):119074-119074.
[16] Q. Wang, K. Luo, C. Wu, et al. Impact of substantial wind farms on the local and regional atmospheric boundary layer: Case study of Zhangbei wind power base in China. ENERGY. 2019;183 (0):1136-1149.
[17] M. Mataji, K. Ashrafi, M. Shafie Pour-Motlagh. Can wind turbine farms increase settlement of particulate matters during dust events? Journal of Renewable and Sustainable Energy. 2023;15(1)
[18] Wang Qiang. Study on mesoscale numerical simulation of wake effect of wind farm & its impact on atmospheric environment. 2020. Zhejiang University, PhD dissertation.
[19] J. Mo, T. Huang, X. Zhang, et al. Spatiotemporal distribution of nitrogen dioxide within and around a large-scale wind farm–a numerical case study. ATMOSPHERIC CHEMISTRY AND PHYSICS. 2017;17 (23):14239-14252.
[20] Z. Li, J. Ni, X. Liu. Sand Collection Efficiency of Vertical Lattice Sand Collectors. Journal of Sediment Research 2003, (01):24-32.
[21] J. Ni, Z. Li, Experimental study on the vertical distribution of sediment transport rate in sediment-laden air flow. Journal of Sediment Research, 2002, (01): 30-35.
[22] Z. Li, D. He. Reviews of fluid dynamics researches in wind energy. Advances in Mechanics. 43.05 (2013):472-525.
[23] P. Wang, W. Hu, X. Zheng. Saltation and Suspension of Sand Particles. Science China (Series G: Physics, Mechanics & Astronomy) 07 (2008):908-918.